Nature of Low-Lying Excited States in H-Aggregated Perylene Bisimide Dyes: Results of TD-LRC-DFT and the Mixed Exciton Model

ARTICLE *in* THE JOURNAL OF PHYSICAL CHEMISTRY B · NOVEMBER 2009

Impact Factor: 3.3 · DOI: 10.1021/jp9061972 · Source: PubMed

Nature of Low-Lying Excited States in H-Aggregated Perylene Bisimide Dyes: Results of TD-LRC-DFT and the Mixed Exciton Model

Fei Pan, Fang Gao, and WanZhen Liang*

Hefei National Laboratory for Physical Science at Microscale, and Department of Chemical Physics, University of Science and Technology of China, Hefei 230026, P. R. China

Yi Zhao†

State Key Laboratory of Physical Chemistry of Solid Surfaces, and Department of Chemistry, Xiamen University, Xiamen, 361005, P. R. China

Received: July 1, 2009; Revised Manuscript Received: September 5, 2009

We characterize the nature of the low-lying excited states in H-aggregated perylene bisimide (PBI) dyes in terms of the recently proposed long-range-corrected density functional theory (LRC-DFT) and the mixed intramolecular Frenkel exciton (FE) and the intermolecular charge-transfer exciton (CTE) model. The singlet vertical excitation energies of H-aggregated PBI dimers and multimers are theoretically evaluated by considering the aggregation details. It is found that the dimer absorption follows closely the spectra of PBI aggregates in solution and demonstrates strong mixing of two kinds of excitons. The experimentally observed low-energy absorption peak near 2.3 eV should not be a pure CT state but a mixed excitonic state. To model the electronic excitations of H-aggregated PBI multichromophoric oligomers, we adopt a mixed FE-CTE model Hamiltonian, whose microscopic parameters are determined from LRC-DFT/TD-LRC-DFT calculations performed on an individual chromophore or a chromophore pair. By involving four to five PBI chromophores, we have succeeded in reproducing the experimental trends of optical properties in PBI stacking, such as the large blue shift of the absorption band, the mixed FE-CTE nature of the low-energy absorption bands, and the large Stokes shift of emission spectra. The long-range correction on DFT exchange-correlation energy functionals is crucial to correctly evaluate the photophysical characteristics of $\pi-\pi$ stacks.

I. Introduction

The photophysical properties of multichromophoric systems, for example, molecular crystals, aggregates, biological light-harvesting complexes, and organic nanostructures, have been the subject of numerous investigations. The description of elementary electronic excitations of multichromophoric systems is greatly simplified when the chromophores have nonoverlapping charge distributions. In such a case, crystal states can be constructed from superpositions of neutral Frenkel exciton (FE) states.[1,2] However, when one goes from dilute solutions to organic molecular solid states, especially the organic functional π-conjugated systems with high charged carrier mobilities, significant overlap between frontier orbitals on adjacent chromophores leads to through-space intercenter full charge delocalization in the stacking direction. The intermolecular charge-transfer excitons (CTEs) may play an important role in the performance of the photophysical properties. More complex theoretical models, therefore, are required to account for the delocalized electrons and electron−phonon couplings in the materials. The notable examples include Perylene-based materials, such as perylene tetracarboxylic acid (PTCDA) crystals and PBI dyes, a potential component in organic electronics and optoelectronics.

The planar compound, PTCDA or PBI, is regarded as an archetype molecular semiconductor because its crystal contains one-dimensional $\pi-\pi$ stacks of unusually tightly packed chromophores (the interplanar distance of only ∼3.3 Å) that facilitate a high degree of π-orbital overlap between adjacent molecules along the stacking direction. Novel properties emanate from such packing features. The experimental studies have suggested the formation of photoluminescent CTEs and the possibility of a significant electro-absorption signal (together with a raise in photocurrent).[3] Extensive theoretical studies have also been conducted,[4–14] with use of the model Hamiltonian or the time-dependent density functional theory (TD-DFT) with the popular hybrid exchange-correlation (XC) functional B3LYP.[15] Those theoretical studies have revealed the importance of the intermolecular CTEs for the optical absorption and emission, assigned the lowest CTE state to lie below the lowest intramolecular FE state, and placed the CTE energy within a wide range of about 2.0−2.5 eV with respect to the different methods.[13,14,16–18] This assignment is unusual in contrast to other noncovalent complexes.

The optical absorption and emission spectra of the PBI monomer and its H-dimer have been experimentally measured[6,7] (see Figure 1 in the Supporting Information). The PBI monomer has the strong low-energy absorption band near 517−527 nm (2.40−2.35 eV), which corresponds to the 0−0 vibrational transition between the electronic ground state and the S_1 excited state, while the H-aggregated dimer shows an intensive absorption band near 491 nm (2.53 eV) and a shoulder near 535 nm (2.32 eV). The origin of the strong blue-shift peak at 2.53 eV is well understood, and it mainly comes from the electronic transitions from the vibronic level $\nu = 0$ of the ground state to the vibronic level $\nu' = 0$ of the upper mixed bright exciton

* Corresponding author. E-mail: liangwz@ustc.edu.cn.
† E-mail address: yizhao@xmu.edu.cn.

10.1021/jp9061972 CCC: $40.75
Published on Web 10/13/2009

state of the dimers. However, previous work on the nature of the low-energy peak at 2.32 eV has been controversial. For instance, Forrest et.al.[5] assigned the low-energy absorption at 2.23 eV of PTCDA films to a novel CT exciton and modeled it with a hydrogenic 1 s radius of 12 Å. Hennessy and his coworkers[16] found that the in-plane polarization matches unpolarized film spectra by measuring the polarized absorption spectrum of a PTCDA single crystal at 300 K, although the feature of the low-energy peak is less resolved and negligible absorption for light normal to the molecular plane is incompatible with almost isotropic absorption in a hydrogenic model. They thus concluded that the spectra within 2−3 eV have the characters of mixed Frenkel-CT excitons. To further clarify these issues, therefore, a reliable electronic structure study on the nature, the splitting, and the energy-level order of excited states is very essential.

Regarding the computational effort involved to study electronic excitation, high accurate ab initio calculations are still challenging for multichromophoric systems with large sizes. Alternatively, TD-DFT provides a practical method to extrapolate ab initio accuracy to molecules of practical interest. However, TD-DFT with the conventional exchange-correction (xc) functionals (even the popular hybrid xc functionals such as B3LYP[15]) has been found to provide a poor description to the large extended π-conjugated systems and long-range intermolecular CT excitations due to the known problems on the nonlocality and asymptotic behavior of available density functionals.[19–21] Motivated by the observation that nonlocal HF exchange potentials properly describe the distance dependence of long-range CT excited states and the dynamic polarizability of extended π-conjugated systems, people incorporate the range-dependent nonlocal HF exchange in the xc functionals and attempt to preserve the form of common GGAs and hybrid functionals at short range while incorporating 100% HF exchange in the long range.[22,23] A range-adjustable parameter, μ, is introduced to determine the length scale over which the HF exchange is turned on in these long-range-corrected DFT schemes.

In the present work, we use the TD-LRC-DFT to explore the electronic excitations of the quasi-one-dimensional H-aggregated PBI dyes. The exciton splitting and the charge-localized CTE energy of dimers calculated by TD-LRC-DFT with the optimal μ value are required to agree with the experimental absorption peak spacing and the CTE energy from the constrained DFT (CDFT) approach,[24] respectively. The low-lying singlet excited states are characterized, and the dependence of exciton energies and exciton splitting on the mutual orientation of single molecules, the intermolecular distances, and the chromophoric sizes are demonstrated. Due to the vital role of CT exciton on the photophysical properties, theoretical studies on the excited states of PTCDA or its derivatives require a calculation involving the multichromophoric system as a supermolecule or using a mixed FE-CTE model. However, even the low-cost TD-DFT approach is still limited to the medium-size systems currently. Thus, for the systems larger than four PBI chromophores, we only use the mixed FE-CTE model whose microscopic parameters are determined from LRC-DFT/TD-LRC-DFT calculations performed on the individual chromophore or chromophore pairs.

The paper is organized as follows. Section II presents the model Hamiltonian and the methods used for the calculation of its microscopic parameters. Section III shows the results of PBI monomers and aggregates from TD-DFT or the mixed FE-CTE model. Detailed discussions and conclusions are given in Section IV.

II. Mixed FE-CTE Model

Considering interchromophore orbital overlap-dependent interactions, the exciton basis set used for calculations needs to be expanded to include CT configurations. For the sake of simplicity, let us consider a bichromophoric system M_aM_b, two intramolecular localized excitations $|M_a^*M_b\rangle$, $|M_aM_b^*\rangle$, and two charge-localized intermolecular excitations $|M_a^+M_b^-\rangle$, $|M_a^-M_b^+\rangle$ which can be formed upon electronic excitation. Two types of electronic configurations mix together to form mixed excitonic states of the bichromophoric system via either purely covalent $\langle M_a^*M_b|H_{DA}|M_aM_b^*\rangle$, ionic (e.g., $\langle M_a^+M_b^-|H_{DA}|M_a^-M_b^+\rangle$), or mixed-type (e.g., $\langle M_a^*M_b|H_{DA}|M_a^+M_b^-\rangle$) interaction.[25,26] The mixed excited states possess the natures of both intramolecular and intermolecular excitations.

The above concept has been specificized as the mixed FE-CTE model, the same as the Merrifield model for Frenkel-CT exciton mixing[27] in a one-dimensional stack. The parametrized Merrifield exciton Hamiltonian includes one electron (position n_e) and one hole (position n_h), which can perform the nearest neighbor hops independently of each other

$$\hat{H} = \hat{H}^{FE} + \hat{H}^{CTE} + \hat{H}^{FC} \tag{1}$$

with

$$\hat{H}^{FE} = \sum_n{}' E_n^F \hat{B}_n^\dagger \hat{B}_n + \sum_{m,n}{}' J_{m,n} \hat{B}_m^\dagger \hat{B}_n,$$

$$\hat{H}^{CTE} = \sum_{n,f}{}' E_f^C \hat{C}_{n,f}^\dagger \hat{C}_{n,f} + \sum_{n,f}{}' [M_h(\hat{C}_{n+1,f-1}^\dagger \hat{C}_{n,f} + \hat{C}_{n-1,f+1}^\dagger \hat{C}_{n,f}) + \text{h.c.}] + \sum_{n,f}{}' [M_e(\hat{C}_{n,f+1}^\dagger \hat{C}_{n,f} + \hat{C}_{n,f-1}^\dagger \hat{C}_{n,f}) + \text{h.c.}],$$

$$\hat{H}^{FC} = \sum_n [t_e(\hat{B}_n^\dagger \hat{C}_{n,+1} + \hat{B}_n^\dagger \hat{C}_{n,-1}) + \text{h.c.}] + \sum_n [t_h(\hat{B}_n^\dagger \hat{C}_{n+1,-1} + \hat{B}_n^\dagger \hat{C}_{n-1,+1}) + \text{h.c.}]$$

Here $\hat{B}_n(\hat{B}_n^\dagger)$ is the annihilation (creation) operator of the electronic excitation on a neutral molecular site n; E^F is the on-site energy of a localized FE; and $J_{m,n}$ is the hopping integral corresponding to excitation transfer from site n to site m. In the summation of H^{FE} (H^{CTE}), the terms for $n = m$ are omitted.

The diagonal element E_m^F of the systematic Hamiltonian H is associated with the diabatic basis wave function $|\Phi_m^i\rangle$ as

$$E_m^F = \langle\Phi_m^i|H|\Phi_m^i\rangle = \langle\Phi_m^i|H_m + \sum_{n\neq m} H_n + \sum_{m,n} V_{mn}|\Phi_m^i\rangle \tag{2}$$

where Φ_m^i denotes the total wave function of the system with the molecule m in its ith excited state Ψ_m^i and all the other molecules in their ground state and V_{mn} is the intermolecular interaction potential of molecule m and n. If the electronic energy of the system composed of all chromophores in the electronic ground state is taken as zero, E_m^F is approximately equal to $\omega_m^i + \Delta D_m$, with ΔD_m corresponding to the gas-to-crystal shift induced by the aggregation.

Under the first-order approximation in the single excitation theory, the coupling between FEs is approximated by[28–30]

$$J_{m,n} = \langle M_m^* M_n | H | M_m M_n^* \rangle \approx \int \mathrm{d}\vec{r} \int \mathrm{d}\vec{r}\,' \rho_m^i(\vec{r}) \left[\frac{1}{|\vec{r} - \vec{r}\,'|} + g_{xc}(\vec{r}, \vec{r}\,') \right] \rho_n^j(\vec{r}\,') - \omega_0 \int \mathrm{d}\vec{r}\, \rho_m^i(\vec{r}) \rho_n^j(\vec{r}) \quad (3)$$

where ρ_m^i and ρ_n^j are the transition densities of the ith excited state of the molecule m and the jth excited state of the molecule n; $g_{xc}(\vec{r}, \vec{r}\,')$ is the exchange-correlation potential; and ω_0 is the transition frequency.

The first sum in $\hat{H}^{\mathrm{CTE}}$ covers the on-site energies of the CT states, which only depend on the separation f. The second sum includes all the nearest neighbor hops of a hole from $n \rightarrow n \pm 1$, and the third sum includes the corresponding hops of an electron from $n + f \rightarrow n + f \pm 1$. The mixing between Frenkel and CT excitons is expressed in the last part of the Hamiltonian. Here, only the transformation of a CT state into any Frenkel state at the site of either a hole or electron is allowed. The relevant transfer integrals t_e (t_h) can be visualized as transfer of an electron (hole) from the excited molecule n to its nearest neighbor. In this work, the vibrational degrees of freedom are not involved for both CT and Frenkel exciton.

The coupling between FE and CTE, $\langle M_m^* M_n | H | M^+ M^- \rangle$ ($\langle M_m M_n^* | H | M^+ M^- \rangle$), is associated with the overlap of the lowest unoccupied orbitals (the highest occupied orbitals) in a single-particle approximation. In this case, the absolute value of the transfer integral for electron (hole) transfer from M_a to M_b is approximately evaluated as

$$t = \frac{\varepsilon_{\mathrm{L+1[H]}} - \varepsilon_{\mathrm{L[H-1]}}}{2} \quad (4)$$

where $\varepsilon_{\mathrm{L[H]}}$ and $\varepsilon_{\mathrm{L+1[H-1]}}$ are the energies of the LUMO and LUMO + 1 [HOMO and HOMO−1] orbitals taken from the closed-shell configuration of the neutral state of the dimer ($M_a M_b$).

III. Results

A. Nature of Low-Lying Excitonic States of H-Aggregated Dimer. To shed some light on how the mixed excitonic states are formed, we consider a coplanar arrangement of two PBI chromophores, separated by an interplanar distance d of 3.72 Å, which corresponds to the shortest interstacking distance. Note that, like the isolated PBI monomer itself, such a coplanar dimer belongs to the C_{2h} symmetry point group.

According to the Frenkel exciton theory, two localized FEs will mix to produce two new delocalized electronic states of the dimer, $|\mathrm{FE}^+\rangle$ and $|\mathrm{FE}^-\rangle$, corresponding to the constructive and destructive linear combination of two FEs, respectively. The state $|\mathrm{FE}^+\rangle$ covers all the oscillator strength. Similarly, two CTE eigenstates of the dimer, $|\mathrm{CT}^+\rangle$ and $|\mathrm{CT}^-\rangle$, can also be represented by the symmetrical and antisymmetrical combinations of two charge-separated CTEs. Only the dimer states which have the same parity mix. The linear combination of $|\mathrm{FE}^+\rangle$ with $|\mathrm{CT}^+\rangle$ leads to two new dipole-allowed excited states with the oscillator strengths along the long molecular axis, one with larger absorption cross-section but weaker CT character and the other with weak absorption cross-section but stronger CT character. The mixing of $|\mathrm{FE}^-\rangle$ with $|\mathrm{CT}^-\rangle$ produces two new dipole-forbidden mixed excitonic states.

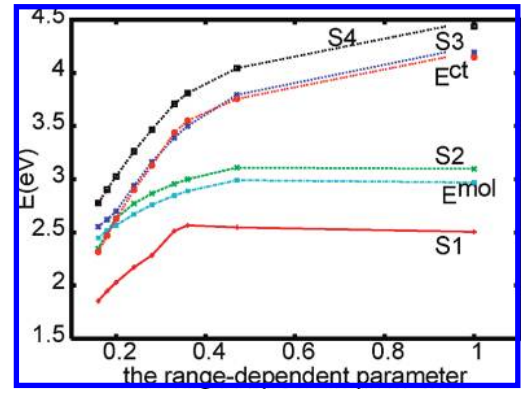

Figure 1. Change of excitation energies of H-aggregated dimer as a function of μ value. The values at $\mu = 1$ denote the TDHF results.

The computational results at the TD-DFT/6-31+G* theory level provide further evidence for the above theoretical prediction. The four low-lying excited states shown in Figure 1 and Table 1 in the Supporting Information, which are fully determined by electronic transitions from two highest occupied molecular orbitals (HOMO) to two lowest unoccupied molecular orbitals (LUMO) of dimer, definitely possess the mixed FE-CTE nature. Here, the popular xc functionals, B3LYP,[15] PBE0[31] and LRC-PBE0, and LRC-Pbeop,[32] are used within the quantum chemistry package Q-chem.[33] Two bright states mainly come from electronic transitions from HOMO (HOMO − 1) → LUMO + 1 (LUMO) of dimer, whereas two dark states come from electronic transitions from HOMO (HOMO − 1) → LUMO (LUMO + 1) of dimer. The contribution of electronic transitions between four pairs of MOs to the four excited states depends very much on the xc functionals. When the xc functionals include smaller components of the HF exchange term, such as B3LYP ($C_{\mathrm{HF}} = 0.2$), PBE0 ($C_{\mathrm{HF}} = 0.25$), and LRC-Pbeop with ($\mu \leq 0.22 a_0^{-1}$), TD-DFT results show that the lower-energy dark state mainly comes from the electronic transition from the HOMO of the supersystem to the LUMO of the supersystem. This one excitation amplitude accounts for more than ∼94% of the norm of the TD-DFT eigenvector, while the electronic transition from HOMO − 1 → LUMO + 1 dominates the contribution to the higher-energy dark state.

The mixing degree, the energy-level order, and the dark/bright exciton splitting of dimer are determined by the energy values of FE and CTE. The lowest CTE states from TD-B3LYP,[15] TD-PBE0,[31] and TD-LRC-Pbeop ($\mu \leq 0.20$) lie below that of the first excited-state of monomer (denoted as $1B_u^{\mathrm{mo}}$). This leads to the lowest dipole-forbidden excited state to have much lower excitation energy than that of the $1B_u^{\mathrm{mo}}$ state, and the bright states with weak oscillator strength (denoted as $1B_u^{\mathrm{di}}$) lie below the one with strong oscillator strength (denoted as $2B_u^{\mathrm{di}}$). When the contribution of HF exchange term increases, such as C_{HF} changes from 0.20 in B3LYP to 0.50 in the 50−50 functional or μ increases from 0.18 to $0.22 a_0^{-1}$ in LRC-Pbeop,[32] we observe that the oscillator strength of $1B_u^{\mathrm{di}}$ states drastically increases and that of $2B_u^{\mathrm{di}}$ states decreases. Both states finally exchange the energy-level order at $u \approx 0.21 a_0^{-1}$. At this point, one observes the smallest energy difference, but the maximum mixing degree between FEs and CTEs.

Figure 2 depicts the change of excitation energies as a function of d at TD-LRC-Pbeop ($\mu = 0.24 a_0^{-1}$) (also see Table 2 in the Supporting Information). The energy of the charge-separated CTE (denoted by E^{C}) increases explicitly and the mixing degree between the lowest FE and CTE decreases as d increases. The decreasing mixing degree between FEs and CTEs

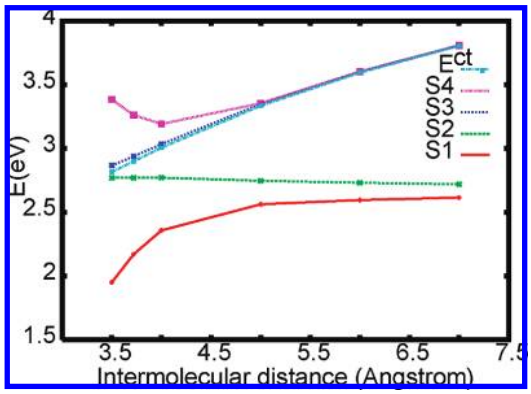

Figure 2. Change of excitation energies of H-aggregated dimer as a function of the interplanar distance *d*.

is evidenced by the decreasing oscillator strength of the $2B_u^{di}$ state and the reducing values of exciton coupling and charge transfer integrals. As $d \geq 5$ Å, the mixing between the lowest FE and the CTE starts to disappear. The Frenkel exciton model alone is efficient to predict the nature of the two lowest excited states of the dimer.

B. Optimal μ Value for PBI H-Dimer. From the above results, we note that both the CT states and the valence states are sensitive to xc functionals or the value of the range-dependent parameter μ. A crucial question arising is how to choose the suitable μ value. In this work, we determine the optimal μ value according to the experimental optical spectra of the parallel H-dimer[6,7] and the energy of charge-separated CTE with respect to different approaches.

Since the mutual orientation of single molecules strongly influences charge and energy transport of the complexes, we investigate the vertical excitation energies of H-dimers at four different conformations (see Figure 2 in the Supporting Information). Conformations H_1 and H_2 correspond to the optimized local minima at the ωB97X-D/6-31+G** level. ωB97X-D[23] is a LRC-DFT scheme with the vdW interaction involved. The structure H_1 lies at $\theta \sim 29.7°$, $d \sim 3.3$ Å, $L = 0$, and the structure H_2 lies at $\theta \sim 26.1°$, $d \sim 3.3$ Å, and $L \sim \pm 1.1$ Å. Here θ, d, and L denote the interplanar rotational displacement, the interplanar distance, and intermolecular longitudinal displacement, respectively. The molecular planes in the conformations H_3 and H_4 are constrained to be strictly perpendicular and parallel to each other with $d = 3.5$ Å, respectively.

Table 1 lists the vertical excitation energies of the four low-lying singlet excited states originated from the electronic transitions from the two highest occupied orbitals to the two lowest unoccupied orbitals of dimer. Obviously, for H_1 and H_2, all the four states produced by TD-DFT are dipole-allowed, and they are sensitive to xc functionals or the μ value. Since the four states in Table 1 are formed by mixing FE and CTE, one may obtain the functional-dependent CTE energies for the structures H_3 and H_4 at the TD-DFT level. It is found that the results produced by TD-LRC-Pbeop ($\mu \sim 0.22a_0^{-1}$, $C_{HF} = 0$) and TD-LRC-Pbe0 ($\mu \sim 0.16a_0^{-1}$, $C_{HF} = 0.25$) agree well with those from the CDFT approach.[24] CDFT predicts an adiabatic CTE energy of 2.86 and 2.62 eV for the dimers H_3 and H_4 at the PBE/6-311G** theory level, respectively. However, considering that the energies of valence states have been overestimated 0.2−0.3 eV by TD-LRC-DFT, we therefore assume that the CTE energies produced by TD-LRC-DFT should be 0.2−0.3 eV larger than these produced by the CDFT approach. Finally, we conclude that the optimal parameter sets for the present system are TD-LRC-PBEh ($\mu = 0.20a_0^{-1}$, $C_{HF} = 0.20$), TD-LRC-Pbeop ($\mu \sim 0.25a_0^{-1}$, $C_{HF} = 0$), and TD-ωB97X-D ($\mu \sim 0.20a_0^{-1}$, $C_{HF} = 0.222$). TD-LRC-Pbeh ($C_{HF} = 0.20$, $\mu \sim 0.20a_0^{-1}$) is suggested by Herbert and co-workers at the hybrid xc functional PBE level to reproduce the SAC−CI potential energy curve for the CT excitation in the $C_2H_4-C_2F_4$ heterodimer.[37]

In Table 1, we also list the values of electronic couplings. It is found that the weakest (strongest) couplings take place in the dimers H_3 (H_4). Thus, two near degenerate high-lying energy states (the third and fourth states) in H_3 are nearly pure CTE states. We take their values as the CTE energies.

TD-LRC-Pbeh ($\mu \sim 0.20a_0^{-1}$, $C_{HF} = 0.20$), TD-LRC-Pbeop ($\mu \sim 0.25a_0^{-1}$, $C_{HF} = 0$), and TD-ωB97X-D ($\mu \sim 0.20a_0^{-1}$, $C_{HF} = 0.222$) produce two distinctly dipole-allowed excited states with the local minima H_1 and H_2, the state with weaker oscillator strength lying ~0.1 eV above the brightest excited state. There is an energy spacing of ~ 0.25−0.3 eV between the two lowest excited states. Taking into account the calculated excited-state energy spacing and the effect of exciton−phonon coupling together, we assign that the band at 491 nm in the experimental absorption spectra of the dimer is mainly originated from the transition from the vibronic state $\nu = 0$ of the ground state to $\nu' = 0$ of the brightest exciton state, and that the band at 530 nm comes from the transition $\nu = 0$ to $\nu' = 1$ of the lowest exciton state. This assignment to the band at 530 nm relies on the facts that the absorption line-shapes of molecules are predominantly determined by the electron populations in the lowest vibronic state of the ground state and that the strong exciton−phonon coupling leads to the vibronic energy spacings of the complex's exciton state alter, and the energy difference between $\nu' = 0$ and $\nu' = 1$ reduces. The parity-allowed transition from $\nu = 0$ of the ground state to $\nu' = 1$ of the first singlet exciton state in H-aggregated dimers becomes observable.[34]

C. Size Dependence of the Dark/Bright Excitons. To simulate how the spectra evolve as the number of PBI chromophores increases, we calculate the spectrum of a one-dimensional coplanar arranged H-aggregated PBI multichromophoric oligomer with the nearest neighbor interplanar distance $d = 3.72$ Å. The calculated results based on TD-LRC-DFT and the mixed FE-CTE model are shown in Table 2 and Figure 3. It is found that both dipole-allowed bright states $1B_u^{mc}$ and $2B_u^{mc}$ of multimers slightly blue-shift, and the energy spacing between the first singlet excited state and the brightest state increases as the number of chromophores increases. The optical gap nearly achieves saturated as the number of PBI chromophores reaches 5−6. It indicates that the excitons are localized in a small region in the one-dimensional H-aggregated PBI oligomer.

We also note that the lowest excited state, labeled with $3B_u$ in the trimer spectra, starts to possess the oscillator strength. This lowest excited state may play a key role in photoluminescence spectra of aggregated PBIs. The experiments have shown that the photoluminescence spectra of PBI aggregates exhibit a significant Stokes shift of ~0.6 eV, and the wide and strong fluorescence emission band centers among 630−700 nm which indicates the existence of self-trapped exciton. Both the Frenkel exciton and the self-trapped exciton can contribute to photoluminescence. In the presence of a barrier between the lowest available states for both of them, the Frenkel exciton is observed as a band with a small Stokes shift, while the self-trapped exciton corresponds to a larger Stokes shift and a broadband. When two neighboring PBI planes strictly parallel each other, our calculations show that the energy difference between the brightest singlet excited state and the lowest singlet excited state is larger than the experimental measured Stokes shift of 0.6

TABLE 1: Vertical Excitation Energies of PBI Dimers at Different Conformations[a]

	xc	S_1	S_2	S_3	S_4	$\|2t_h\|$	$\|2t_e\|$	$\|2J\|$	E^{mol}	E^{cT}
H_1	Pbeop(0.20)	2.4123(0.031)	2.6616(0.069)	2.7376(0.016)	2.7552(0.896)	0.129	0.085	0.247		
	Pbeop(0.22)	2.4839(0.035)	2.7798(0.443)	2.8304(0.560)	2.8593(0.013)	0.130	0.085			
	Pbeop(0.24)	2.5509(0.039)	2.8503(0.913)	2.9380(0.107)	2.9776(0.012)	0.131	0.085			
	Pbeop(0.33)	2.7694(0.044)	3.0536(1.111)	3.3240(0.011)	3.3868(0.016)	0.191	0.136			
	ωB97X-D	2.6141(0.044)	2.9125(1.003)	3.0190(0.079)	3.0582(0.012)	0.135	0.087	0.269		
	Pbe0	2.1229(0.008)	2.1985(0.001)	2.4385(0.037)	2.6450(0.912)	0.109	0.082			
	LR-Pbe0(0.16)	2.5158(0.038)	2.7937(0.170)	2.8622(0.844)	2.8769(0.018)	0.137	0.092			
H_2	Pbeop(0.20)	2.4102(0.027)	2.6067(0.143)	2.6436(0.006)	2.7193(0.813)	0.082	0.030	0.239		
	Pbeop(0.22)	2.4750(0.029)	2.7174(0.469)	2.7702(0.005)	2.8021(0.525)	0.082	0.027			
	Pbeop(0.24)	2.5302(0.030)	2.7936(0.818)	2.8863(0.004)	2.9037(0.216)	0.083	0.028			
	ωB97X-D	2.5805(0.032)	2.8315(0.835)	2.9657(0.003)	2.9980(0.249)	0.084	0.028	0.261		
	Pbe0	2.1214(0.003)	2.1536(0.003)	2.3407(0.028)	2.595(0.919)	0.082	0.027			
	LR-Pbe0(0.15)	2.4761(0.027)	2.6816(0.150)	2.7192(0.007)	2.7963(0.856)	0.082	0.027			
	LR-Pbeh(0.20)	2.5662(0.032)	2.8320(0.789)	2.9199(0.004)	2.9360(0.270)	0.089	0.034			
H_3	Pbeop(0.20)	2.5331(0.499)	2.5342(0.501)	2.8079(0.014)	2.8087(0.014)	0.054	0.0	0.004		
	Pbeop(0.24)	2.6404(0.542)	2.6418(0.544)	3.0878(0.007)	3.0886(0.007)	0.054	0.0	0.004	2.6711(0.759)	3.0878
	Pbeop(0.33)	2.8170(0.602)	2.8182(0.603)	3.5504(0.004)	3.5514(0.041)	0.054	0.0		2.8646(0.837)	3.5507
	ωB97X-D	2.6889(0.558)	2.6902(0.559)	3.1508(0.007)	3.1517(0.007)	0.054	0.0	0.004	2.7235(0.780)	3.1513
	Pbe0	2.1556(0.006)	2.1563(0.006)	2.4389(0.478)	2.4399(0.479)	0.054	0.0			
	LR-Pbe0(0.16)	2.6264(0.527)	2.6274(0.529)	2.9232(0.013)	2.9241(0.013)	0.056	0.0			
H_4	Pbeop(0.20)	1.8103(0.0)	2.5799(0.107)	2.6878(0.977)	3.1575(0.0)	0.640	0.680		2.5664(0.710)	2.5528
	Pbeop(0.24)	1.9508(0.0)	2.7714(0.975)	2.8667(0.184)	3.3845(0.0)	0.653	0.708	0.269	2.6711(0.759)	2.8169
	Pbeop(0.30)	2.1131(0.0)	2.9118(1.236)	3.1734(0.027)	3.6674(0.0)	0.707	0.735	0.279	2.7968(0.815)	3.1361
	ωB97X-D	1.9886(0.0)	2.8278(1.063)	2.9414(0.134)	3.4690(0.0)	0.682	0.729	0.270	2.7235(0.780)	2.8899
	Pbe0	1.5284(0.0)	2.0951(0.003)	2.5813(1.020)	2.8302(0.0)	0.626	0.653		2.4652(0.669)	2.0532
	LR-Pbe0(0.16)	1.8681(0.0)	2.7028(0.205)	2.7937(0.950)	3.3141(0.0)	0.680	0.734		2.6621(0.748)	2.6773

[a] H_1: $\theta = 29.7°$, $L = 0$, and $d = 3.3$ Å. H_2: $\theta = 26.7°$, $L = 1.1$ Å, and $d = 3.3$ Å. H_3: $\theta = 90.0°$, $L = 0$, and $d = 3.5$ Å. H_4: $\theta = 0$, $L = 0$, and $d = 3.5$ Å. The values in parentheses denote the oscillator strength. E^{mol} and E^{ct} denote the first excited-state energy of monomer and the CTE energy of dimers.

TABLE 2: Vertical Excitation Energies of PBI Multimers As a Function of Aggregated Sizes Produced by TD-LRC-DFT and the Mixed Exciton Model[a]

NC	HOMO	LUMO	S_1	S_2	S_3	S_4	S_5	S_6	S_7
					Pbeop ($\mu = 0.20a_0^{-1}$)				
1	−0.283	0.091	2.5664	3.5157					
2	−0.2776	−0.103	2.0293(0.0)	2.6329(0.475)	2.6981(0.621)	0.0262(0.0)	3.3913(0.0)		
			[2.0493	2.6203 ($1B^{di}$)	2.6982 ($2B^{di}$)	3.0192]			
3	−0.276	−0.109	1.8773(0.004)	2.2231(0.0)	2.5533(0.0)	2.6431(0.240)	2.7347(1.200)	2.9255(0.0)	3.0105(0.002)
			[1.9269 ($3B^{tri}$)	2.2340	2.6224	2.6271 ($1B^{tri}$)	2.7660 ($2B^{tri}$)	2.9159	3.1151]
4	−0.276	−0.112							
			[1.900 ($3B^{qua}$)	2.1012	2.3810	2.6244	2.6271 ($1B^{qua}$)	2.7731 ($2B^{qua}$)	2.8234]
5	−0.276	−0.114							
					Pbeop ($\mu = 0.24a_0^{-1}$)				
1	−0.290	−0.087	2.6711	3.6873					
2	−0.285	−0.100	2.1710(0.0)	2.7710(1.128)	2.9387(0.054)	2.3626(0.0)	3.4559(0.0)		
			[2.1963	2.7945 ($1B^{di}$)	2.9051 ($2B^{di}$)	3.2474]			
3	−0.283	−0.106	2.0244(0.005)	2.3715(0.0)	2.8178(0.0)	2.8209(1.401)	2.9396(0.179)	3.1549(0.0)	3.2440(0.002)
			[2.0728 ($3B^{tri}$)	2.3842	2.8596	2.9006 ($1B^{tri}$)	2.9162 ($2B^{tri}$)	3.1375	3.3448]
4	−0.283	−0.109							
			[2.0457 ($3B^{qua}$)	2.2421	2.5384	2.8832	2.9006 ($1B^{qua}$)	2.9257 ($2B^{qua}$)	3.0363]
5	−0.283	−0.111							
					ωB97X-D ($\mu = 0.20a_0^{-1}$, $C_{HF} = 0.22$)				
1	−0.296	−0.091	2.7235	3.7795					
2	−0.290	−0.103	2.2154(0.0)	2.8252(1.177)	3.0115(0.046)	3.3418(0.0)	3.5280(0.0)	3.7091(0.0)	
			[2.2412	2.8480 ($1B^{di}$)	2.9779 ($2B^{di}$)	3.3268]			
3	−0.288	−0.109	2.0563(0.006)	2.417(0.0)	2.8780(1.465)	2.8820(0.0)	3.0110(0.146)	3.1900(0.0)	
			[2.1148 ($3B^{tri}$)	2.4327	2.9166 ($1B^{tri}$)	2.9735	2.9735	2.9864 ($2B^{tri}$)]	
4			[2.0642 ($3B^{qua}$)	2.2535	2.5760	2.9355 ($1B^{qua}$)	2.9735	2.9735	2.9951 ($2B^{qua}$)]

[a] The values in parentheses denote the oscillator strength, and those in brackets denote the results based on the mixed FE-CTE model.

eV. However, the difference reduces as the neighboring intermolecular rotational angles increase. Therefore, by taking into account the gas-to-crystal shift induced by the aggregation, the reorganization energy, the overestimated excitation energies by TD-LRC-DFT, and the fact that there is an interplanar rotational displacement upon photoexcitation on PBI aggregates, we may expect that this lowest singlet excited state is in very close agreement with the strongest fluorescence emission band. Our theoretical calculations based on the mixed FE-CTE model have achieved a satisfactory agreement with the experiment.

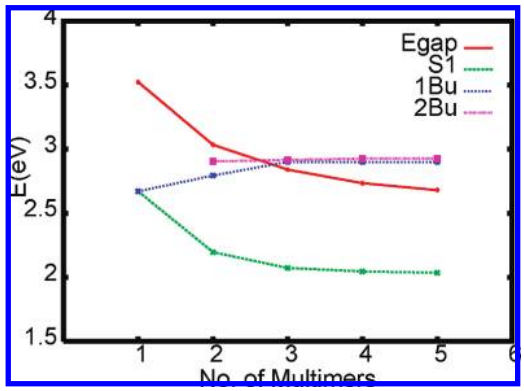

Figure 3. Change of excitation energies of H-aggregated dimer as a function of the number of multimers.

IV. Concluding Remarks

By using both TD-LRC-DFT and the mixed FE-CTE model, we study the low-lying excited states of H-aggregated PBI dyes. The following conclusions can be drawn from this research work.

(1) The effect of the long-range correction on DFT xc functionals is crucial for noncovalent systems.

The conventional hybrid xc functionals B3LYP and PBE0 underestimate the energy of the intermolecular charge-transfer excited states. For the present system, the lowest CTE energies produced by TD-B3LYP and TD-PBE0 are even less than the previously published values.[13,17,18] Implementing the range-dependent nonlocal HF exchange potential on DFT xc functionals is crucial to correctly describe the intermolecular CT excitation of $\pi-\pi$ stacking. However, we find that several previously optimized μ values[35,36] using ground-state benchmarks including atomization energies and barrier heights are too large to study the electronic excitation of nonconvalent large-size π-conjugated systems. The parameter sets TD-LRC-Pbeop ($C_{HF} = 0.0$, $\mu \sim 0.25a_0^{-1}$), TD-LRC-Pbeh ($C_{HF} = 0.20$, $\mu \sim 0.20a_0^{-1}$), and TD-ωB97X-D ($C_{HF} = 0.22$, $\mu \sim 0.20a_0^{-1}$) are suitable for the present systems.

(2) The low-lying excited states possess both the nature of CTE and FE.

The CT exciton has a significant contribution on the photophysical properties of the $\pi-\pi$ stacked PBI aggregates. The energy of CTE should be slightly higher than that of the lowest-energy FE, which is just the reason that the strong mixing between FE and CTE takes place and the low-lying excited states possess both the nature of FE and CTE. Therefore, to correctly describe the electronic excitation and emission of $\pi-\pi$ stacked PBI dyes, one should go beyond the Frenkel exciton model.

(3) The strong exciton−phonon coupling induces the appearance of low-energy absorption and emission bands.

We assign the experimentally measured low-energy absorption peak at 2.32 eV originated from the electronic transition from the vibronic state $\nu = 0$ of the ground state to $\nu' = 1$ of the lowest singlet exciton state formed by the linear combination of $|FE^-\rangle$ and $|CTE^-\rangle$. This assignment is based on the fact that there is the strong exciton−phonon coupling in the system. The exciton−phonon coupling leads to the vibronic energy spacings of the complex's exciton state alter. The state $\nu' = 1$ gets closer to the state $\nu' = 0$. Finally, the parity-allowed transition from $\nu = 0$ of the ground state to $\nu' = 1$ of the first singlet exciton state in H-aggregated multimers becomes observable.[34]

Photoabsorption in the H-aggregates leads preferentially to the brightest state ($1B_u^{mc}$), while the excitation to other states has a lower probability. The population in the $1B_u^{mc}$ state is rapidly transferred to the lower exciton state via the conical intersection. However, at very low temperature such as $T = 0$ K, the transferred electron mainly populated on the vibronic state $\nu' = 0$ of the lowest exciton state. Since the electron transition from $\nu' = 0 \rightarrow \nu = 0$ is almost dipole-prohibited, we will not observe the strong fluorescence emission from the lower exciton state. However, the strong exciton−phonon coupling leads to the energy spacing of the lowest two vibronic states to shrink, and the thermal population on the higher vibronic state becomes possible at the higher temperature. The parity-allowed transition, from $\nu' = 1$ of the lowest exciton state to $\nu = 0$ of the ground state, makes the low-energy dark state in H-aggregated multimers become pronouncedly observable.[34] This explanation is supported by the calculated energy difference between the brightest state ($1B_u^{mc}$) and the lowest singlet states, which is close to the experimentally measured large Stokes shift.

Acknowledgment. Financial support from National Science Foundation of China (Nos. 20673104, 20833003, and 20833004), a 973 project funded by National Basic Research Program of China (Nos: 2004CB719901 and 2006CB922004), and Chinese Academy of Science is acknowledged.

Supporting Information Available: The geometries, the vertical excitation energies of PBI dimers with respect to a series of DFT functionals and the experimental optical spectra of PBI dyes are supplemented. This material is available free of charge via the Internet at http://pubs.acs.org.

References and Notes

(1) (a) Mukamel, S.; Abramavicius, D. S. *Chem. Rev.* **2004**, *104*, 2073. (b) Spano, F. C. *Annu. Rev. Phys. Chem.* **2006**, *57*, 217. (c) Bredas, J.-L.; Beljonne, D.; Coropceanu, V.; Cornil, J. *Chem. Rev.* **2004**, *104*, 4971. (d) May, V.; Kühn, O. *Charge and Energy Transfer Dynamics in Molecular Systems*, Wiley-VCH: 2005. (e) Schwartz, B. J. *Annu. Rev. Phys. Chem.* **2003**, *54*, 141.

(2) (a) Krueger, B. P.; Scholes, G. D.; Fleming, G. R. *J. Phys. Chem. B* **1998**, *102*, 5378. (b) Scholes, G. D.; Fleming, G. R. *J. Phys. Chem. B* **2000**, *104*, 1854. (c) Scholes, G. D.; Jordanides, X. J.; Fleming, G. R. *J. Phys. Chem. B* **2001**, *105*, 1640. (d) Jordanides, X. J.; Scholes, G. D.; Fleming, G. R. *J. Phys. Chem. B* **2001**, *105*, 1652.

(3) (a) Shen, Z.; Burrows, P. E.; Forrest, S. R.; Ziari, M.; Steier, W. H. *Chem. Phys. Lett.* **1995**, *236*, 129. (b) Bulovic, V.; Burrows, P. E.; Forrest, S. R.; Cronin, J. A.; Thompson, M. E. *Chem. Phys.* **1996**, *210*, 1. (c) Forrest, S. R. *Chem. Rev.* **1997**, *97*, 1793.

(4) (a) Würthner, F. *Chem. Commun.* **2004**, 1564. (b) Langhals, H. *Helv. Chim. Acta* **2005**, *88*, 1309. (c) Wasielewski, M. R. *J. Org. Chem.* **2006**, *71*, 5051. (d) Elemans, J. A. A. W.; van Hameren, R.; Nolte, R. J. M.; Rowan, A. E. *Adv. Mater.* **2006**, *18*, 1251.

(5) Forrest, S. R. *Chem. Rev.* **1997**, *97*, 1793.

(6) Yagai, S.; Seki, T.; Karatsu, T.; Kitamura, A.; Würthner, F. *Angew. Chem., Int. Ed.* **2008**, *47*, 3367.

(7) (a) Giaimo, J. M.; Lockard, J. V.; Sinks, L. E.; Scott, A. M.; Wilson, T. M.; Wasielewski, M. R. *J. Phys. Chem. A* **2008**, *112*, 2322. (b) Ahrens, M. J.; Goshe, A. J.; Tiede, D. M.; Gusev, A. V.; Giaimo, J. M.; Jones, B. A.; Liu, W.; Rybtchinski, B.; Sinks, L. E.; Wasielewski, M. R. *J. Am. Chem. Soc.* **2004**, *126*, 8284.

(8) Chen, Z.; Stepanenko, V.; Dehm, V.; Prins, P.; Siebbeles, L. D. A.; Seibt, J.; Marquetand, P.; Engel, V.; Würthner, F. *Chem.—Eur. J.* **2007**, *13*, 436.

(9) Clark, A. E.; Qin, C.-Y.; Li, A. D. Q. *J. Am. Chem. Soc.* **2007**, *129*, 7586.

(10) Li, A. D. Q.; Wang, W.; Wang, L.-Q. *Chem.—Eur. J.* **2003**, *9*, 4594. Wang, W.; Li, L. S.; Helms, G.; Zhou, H. H.; Li, A. D. Q. *J. Am. Chem. Soc.* **2003**, *125*, 1120.

(11) Reinhold, F. F.; Seibt, J.; Engel, V.; Renz, M.; Kaupp, M.; Lochbrunnerä, S.; Zhao, H.-M.; Pfister, J.; Wüthner, F.; Engels, B. *J. Am. Chem. Soc.* **2008**, *130*, 12858.

(12) (a) Seibt, J.; Marquetand, P.; Engel, V.; Chen, Z.; Dehm, V.; Würthner, F. *Chem. Phys.* **2006**, *328*, 354. (b) Chen, Z.; Stepanenko, V.; Dehm, V.; Prins, P.; Siebbeles, L. D. A.; Seibt, J.; Marquetand, P.; Engel, V.; Würthner, F. *Chem.—Eur. J.* **2007**, *13*, 436.

(13) Scholz, R.; Kobitski, A. Y.; Zahn, D. R. T.; Schreiber, M. *Phys. Rev. B* **2005**, *72*, 245208.

(14) (a) Hoffmann, M.; Soos, Z. G. *Phys. Rev. B* **2002**, *66*, 024305. (b) Kazmaier, P. M.; Hoffmann, R. *J. Am. Chem. Soc.* **1994**, *116*, 9684. (c) Haskal, E. I.; Shen, Z.; Burrows, P. E.; Forrest, S. R. *Phys. Rev. B* **1995**, *51*, 4449. (d) Hoffmann, M.; Schmidt, K.; Fritz, T.; Hasche, T.; Agranovich, V. M.; Leo, K. *Chem. Phys.* **2000**, *258*, 73.

(15) (a) Becke, A. D. *J. Chem. Phys.* **1993**, *98*, 5648. (b) Stephens, P. J.; Devlin, F. J.; Chabalowski, C. F.; Frisch, M. J. *J. Chem. Phys.* **1994**, *98*, 11623.

(16) Hennessy, M. H.; Soos, Z. G.; Pascal, R. A., Jr.; Girlando, A. *Chem. Phys.* **1999**, *245*, 199.

(17) Mazur, G.; Petelenz, P.; Slawik, M. *J. Chem. Phys.* **2003**, *118*, 1423.

(18) Tsiper, E. V.; Soos, Z. G. *Phys. Rev. B* **2001**, *64*, 195124.

(19) Cai, Z.-L.; Sendt, K.; Reimers, J. R. *J. Chem. Phys.* **2002**, *117*, 5543.

(20) (a) Dreuw, A.; Head-Gordon, M. *Chem. Rev.* **2005**, *105*, 4009. (b) Dreuw, A.; Head-Gordon, M. *J. Am. Chem. Soc.* **2004**, *126*, 4007. (c) Dreuw, A.; Weisman, J. L.; Head-Gordon, M. *J. Chem. Phys.* **2003**, *119*, 2943.

(21) Magyar, R. J.; Tretiak, S. *J. Chem. Theory Comput.* **2007**, *3*, 976.

(22) (a) Leininger, T.; Stoll, H.; Werner, H.-J.; Savin, A. *Chem. Phys. Lett.* **1997**, *275*, 151. (b) Toulouse, J.; Colonna, F.; Savin, A. *J. Chem. Phys.* **2005**, *122*, 014110. (c) Ángyán, J. G.; Gerber, I. C.; Savin, A.; Toulouse, J. *Phys. Rev. A* **2005**, *72*, 012510. (d) Goll, E.; Werner, H.-J.; Stoll, H. *Phys. Chem. Chem. Phys.* **2005**, *7*, 3917. (e) Goll, E.; Werner, H.-J.; Stoll, H.; Leininger, T.; Gori-Giorgi, P.; Savin, A. *Chem. Phys.* **2006**, *329*, 276. (f) Iikura, H.; Tsuneda, T.; Yanai, T.; Hirao, K. *J. Chem. Phys.* **2001**, *115*, 3540. (g) Tawada, Y.; Tsuneda, T.; Yanagisawa, S.; Yanai, T.; Hirao, K. *J. Chem. Phys.* **2004**, *120*, 8425. (h) Gerber, I. C.; Ángyán, J. G. *Chem. Phys. Lett.* **2005**, *415*, 100. (i) Gerber, I. C.; Ángyán, J. G.; Marsman, M.; Kresse, G. *J. Chem. Phys.* **2007**, *127*, 054101. (j) Vydrov, O. A.; Heyd, J.; Krukau, A. V.; Scuseria, G. E. *J. Chem. Phys.* **2006**, *125*, 074106. (k) Vydrov, O. A.; Scuseria, G. E. *J. Chem. Phys.* **2006**, *125*, 234109. (l) Song, J.-W.; Hirosawa, T.; Tsuneda, T.; Hirao, K. *J. Chem. Phys.* **2007**, *126*, 154105. (m) Cohen, A. J.; Mori-Sánchez, P.; Yang, W. *J. Chem. Phys.* **2007**, *126*, 191109. (n) Baer, R.; Neuhauser, D. *Phys. Rev. Lett.* **2005**, *94*, 043002.

(23) (a) Chai, J.-D.; Head-Gordon, M. *J. Chem. Phys.* **2008**, *128*, 084106. (b) Chai, J.-D.; Head-Gordon, M. *Chem. Phys. Lett.* **2008**, *467*, 176. (c) Chai, J.-D.; Head-Gordon, M. *Phys. Chem. Chem. Phys.* **2008**, *10*, 6615.

(24) Wu, Q.; Van, V. T. *J. Chem. Phys.* **2006**, *125*, 164105.

(25) Scholes, G. D.; Harcourt, R. D.; Ghiggino, K. P. *J. Chem. Phys.* **1995**, *102*, 9574.

(26) Thompson, A. L.; Gaab, K. M.; Xu, J.; Bardeen, C. J.; Martinez, T. J. *J. Phys. Chem. A* **2004**, *108*, 671.

(27) Merrifield, R. E. *J. Chem. Phys.* **1961**, *31*, 1835.

(28) McWeeny, R. *Methods of Molecular Quantum Mechanics*, 2nd ed.; Academic Press: London, U.K., 1992.

(29) Hsu, C.-P.; Fleming, G. R.; Head-Gordon, M.; Head-Gordon, T. *J. Chem. Phys.* **2001**, *114*, 3065.

(30) Scholes, G. D. *Annu. Rev. Phys. Chem.* **2003**, *54*, 57.

(31) Adamo, C.; Barone, V. *J. Chem. Phys.* **1999**, *110*, 6158.

(32) Tsuneda, T.; Suzumura, T.; Hirao, K. *J. Chem. Phys.* **1999**, *110*, 10664.

(33) Shao, Y.; Molnar, L. F.; Jung, Y.; Kussmann, J.; Ochsenfeld, C.; Brown, S. T.; Gilbert, A. T. B.; Slipchenko, L. V.; Levchenko, S. V.; O'Neill, D. P.; DiStasio, R. A.; Lochan, R. C.; Wang, T.; Beran, G. J. O.; Besley, N. A.; Herbert, J. M.; Lin, C. Y.; Van Voorhis, T.; Chien, S. H.; Sodt, A.; Steele, R. P.; Rassolov, V. A.; Maslen, P. E.; Korambath, P. P.; Adamson, R. D.; Austin, B.; Baker, J.; Byrd, E. F. C.; Dachsel, H.; Doerksen, R. J.; Dreuw, A.; Dunietz, B. D.; Dutoi, A. D.; Furlani, T. R.; Gwaltney, S. R.; Heyden, A.; Hirata, S.; Hsu, C. P.; Kedziora, G.; Khalliulin, R. Z.; Klunzinger, P.; Lee, A. M.; Lee, M. S.; Liang, W.; Lotan, I.; Nair, N.; Peters, B.; Proynov, E. I.; Pieniazek, P. A.; Rhee, Y. M.; Ritchie, J.; Rosta, E.; Sherrill, C. D.; Simmonett, A. C.; Subotnik, J. E.; Woodcock, H. L.; Zhang, W.; Bell, A. T.; Chakraborty, A. K.; Chipman, D. M.; Keil, F. J.; Warshel, A.; Hehre, W. J.; Schaefer, H. F.; Kong, J.; Krylov, A. I.; Gill, P. M. W.; Head-Gordon, M. *Phys. Chem. Chem. Phys.* **2006**, *8*, 3172.

(34) Gao, F; Liang, W. Z.; Zhao Y. *J. Phys. Chem. A*, accepted.

(35) Song, J.-W.; Hirosawa, T.; Tsuneda, T.; Hirao, K. *J. Chem. Phys.* **2007**, *126*, 154105.

(36) Vydrov, O. A.; Heyd, J.; Krukau, A. V.; Scuseria, G. E. *J. Chem. Phys.* **2006**, *125*, 074106.

(37) (a) Rohrdanz, M. A.; Herbert, J. M. *J. Chem. Phys.* **2008**, *129*, 034107. (b) Lange, A. W.; Herbert, J. M. *J. Am. Chem. Soc.* **2009**, *131*, 3913.

JP9061972